The Physics and Plasma Chemistry of an RF Needle in a Saltwater Aerosol

W. Lowell Morgan, *Member, IEEE*, and Louis A. Rosocha, *Associate Member, IEEE*

***Abstract*—Experiments involving the insertion of a tungsten needle powered by an ∼1-kW radio-frequency (RF) generator into a flowing saltwater mist produced by a nebulizer are described. The tip of the tungsten electrode is estimated to have a temperature near the 5555-°C vaporization temperature of tungsten. Values of E/N close to the electrode tip are estimated to be greater than the breakdown threshold of humid air. This arrangement of RF-powered electrode and flowing saltwater aerosol produces a flame of some 30 cm high having strong light emission near the 589-nm sodium-D lines. We present a model demonstrating that the emission trapped in the core along the length of the flame arises primarily from $Na(3^2P \rightarrow 3^2S)$ with some Na_2^* emission. The rising flame cools slowly due to a combination of the opacity of the hot gas, the large heat capacity of the H_2O molecules in the flame, and the exothermicity of the plasma chemistry in the afterglow.**

***Index Terms*—Electrical discharges, needles, plasma chemistry, radio frequency (RF), saltwater.**

I. Background

THE EXPERIMENTS described and analyzed herein came about as part of a broader investigation into electric discharges in saltwater aerosols. We have recently published [1] a part of our research having to do with high-voltage and high-current short-pulse surface discharges on saltwater.

Plasmas in the vicinity of radio-frequency (RF) needles have been a subject of research in recent years [2], mostly having to do with potential medical applications. Such experiments typically work at very low power, in flowing rare gases such as helium or argon at atmospheric pressure. The RF is usually the 13.56-MHz industrial standard. The milliwatt-to-watt powers used in the plasma needle experiments reviewed in [2] have negligible thermal emission and evaporation of the needle.

Lazović *et al.* [3] have performed some relatively high-power RF needle experiments with excellent diagnostics. They used a 0.5-mm-diameter tungsten needle mounted coaxially in a tube with flowing He, Ar, and air operating the device at 13.56-MHz RF powers of 10–130 W or about 10% of our RF power. They performed mass spectrometry on the plasma products measuring quantitatively the yields of He^+, Ar^+, N_2^+, O_2^+, N^+, O^+, H_2O^+, N_2O^+, NO^+, CO_2^+, NO, NO_2, and O_3 from the device.

Manuscript received May 17, 2012; revised August 6, 2012; accepted September 12, 2012. Date of publication October 24, 2012; date of current version December 7, 2012.

W. L. Morgan is with Kinema Research & Software, LLC, Monument, CO 80132 USA (e-mail: morgan@kinema.com).

L. A. Rosocha is with Applied Physics Consulting, Los Alamos, NM 87544 USA (e-mail: plasmamon@msn.com).

Color versions of one or more of the figures in this paper are available online at http://ieeexplore.ieee.org.

Digital Object Identifier 10.1109/TPS.2012.2220570

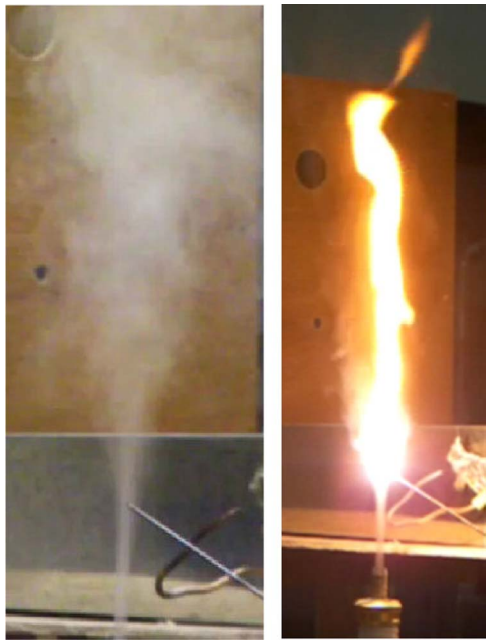

Fig. 1. (a) Geometry of experiment with 35-g/L saltwater mist and 1/16-in Ce/W monopole electrode; (b) 30-cm flame with electrode powered to 1 kW at 13.56 MHz.

In what follows, we briefly describe our experiments using a 1-kW RF needle and devote most of our attention to analyzing and modeling aspects of the plasma physics and chemistry in various regions. This research was an interesting one aside to the more intensive research that we were performing on flowing saltwater mists in a conventional electric arc discharge.

II. Experimental Details

The geometry of our experiment can be seen in Fig. 1. It comprised of a 1/16-in (0.16 cm) 3% Ce/W rod acting as a monopole antenna driven by an ∼1-kW RF source at 13.56 MHz. The tungsten "needle" was inserted into the flowing mist or aerosol from a nebulizer containing a 35-g/L sodium chloride aqueous solution.

The volumetric flow rate of saltwater from the nebulizer was 0.09 mL/s ≃ 0.1 g/s. The i.d. of the exit orifice from the nebulizer was 1/4 in (0.64 cm), and the flow speed was 240 cm/s. The composition of the flow was air saturated with water vapor at 20 °C and saltwater droplets. We will discuss the nature of the saltwater droplets later. Most of the flowing mass was in the saltwater droplets.

Photographs of the operating device are shown in Fig. 1. The first frame shows the aerosol stream and the tungsten needle

operating in air. As expected, the aerosol flow is laminar for a distance before it becomes turbulent. When the needle is operated in air, the electric field at its tip is close to the air breakdown field. The physics of the high-voltage needle plasma in pure air, which exhibits essentially no flame, is similar to that of a corona discharge in the vicinity of the needle point. As described in the following, the physics is very different when the needle is immersed in a flowing saltwater aerosol. We note here that the experiments were performed at an elevation of 7000 ft. The laboratory temperature was 20 °C so the ambient air pressure was 0.77 atm $= 77.8$ kPa.

In the presence of the flowing aerosol, the tungsten needle was much hotter than it was in air alone as evidenced by its evaporation rate of $\sim$1 cm/min indicating a temperature of about 5500 °C, i.e., near the tungsten vaporization temperature. The second frame of Fig. 1 shows the $\sim$30-cm extended flame produced by the RF field. In these experiments, the "flame" is primarily produced by atomic sodium emission from the plasma core that is radiatively trapped and escapes over a long-enough period of time for the hot gas to rise $\sim$30 cm vertically.

In the execution of the experiments, we had little in the way of diagnostics except for our knowledge of the RF power going into the antenna, observations using an optical spectroscope, and high-speed, up to 1000 ft/s, video photography.

III. Physical and Plasma Chemistry

A. Charging of Saltwater Droplets

Based on measurements by Rodes *et al.* [4], we expect the average diameter of the saltwater droplets to be ~ 1 μm. The distribution of diameters is roughly a Gaussian having a full-width at half-maximum of about 1/2 μm.

An interesting aspect of such droplets is that they are likely to be charged. This topic has a long history dating back at least as far as Rayleigh in the 1880s. Unlike simple evaporation of water, which leaves dissolved solids behind, the drops comprising a mist or aerosol are themselves saltwater. As it is very unlikely that each drop would contain identical numbers of Na^+ and Cl^- ions, the drops tend to be charged. This is known as statistical charging. The number of excess ions in each drop is, of course, much less than the total number of ions in the drop. The net charge on each drop can, nevertheless, be the range of 10^5e–10^8e, where $e = 1.6 \times 10^{-19}$ and coulombs is the electronic unit of charge. Very large drops may be highly enough charged to induce a corona discharge around them [5]–[7]. Our $\sim$1-μm-diameter droplets are far too small to form individual droplet corona discharges.

Rayleigh provided a theoretical stability criterion for charged drops, which we will introduce as follows. Zeleny [5], [6], in the early 20th century, observed emission from positive and negative liquid drop electrode points. His work was taken up again some years later by English in 1948 [7]. The field exploded in the 1960s with the development of electrospray ionization (ESI) techniques and ESI mass spectrometry. Blanchard [8]–[10] proposed in the 1950s the creation of charged saltwater drops from bubbles and spray in the sea. Charged water drops have become an important research topic in meteorology [11]–[13].

The study of charged drops falls into two major areas: the creation of charged drops and the mechanisms by which they shed their excess charge.

There are a number of possible mechanisms for the charging of liquid droplets [14]. Leontovich provided in 1946 an expression for the rms net number excess charges of either sign on a droplet. This was used by Iribarne and Thomson [15] in their highly cited 1976 work on ion emission from charged droplets. The Leontovich expression has

$$\langle N_i \rangle_{\rm rms} = \left[\langle N^2 \rangle\right]^{\frac{1}{2}} \propto R^2 N_i \lambda_D$$

where R is the droplet radius; N_i is the total ion density, which is proportional to the molarity of the solution; and $\lambda_D \propto N_i^{-1/2}$ is the Debye length. Brush and Wensrich in 1961 [16] noted that, due to the restriction of the Debye–Huckel model to small electrolyte concentrations, Leontovich's theory is only a valid approximation for an electrolyte density $N_i \ll (\varepsilon kT)^3/8\pi e^6$ or molarity $M \ll 10^{-3}$ mol/L or a Debye length $\lambda_D \gg 10$ nm.

In 1953 work by Dodd [14], he modeled droplet statistical charging as a combinatorial problem involving Bernoulli trials. In a 1:1 electrolyte such as NaCl having equal concentrations of positive and negative ions, the probability that a droplet contains N_i ions of a given charge is given by the binomial distribution. For large values of N_i, the binomial distribution is approximated by a Gaussian distribution. The standard deviation is just $\left[\langle N^2 \rangle\right]^{1/2}$.

B. Disintegration of Charged Saltwater Droplets

Rayleigh studied the stability of charged drops in the 1880s and derived a criterion for the amount of excess charge that a drop of radius R could contain and remain stable. The relationship between the Rayleigh critical charge and the radius is

$$Q_{\rm Rayleigh} = 8\pi(\gamma \varepsilon_o R^3)^{\frac{1}{2}}.$$

If the drop has charge Q and is evaporating so that R is decreasing, at some radius, the repulsive coulombic forces due to the excess ions will overcome the surface tension γ holding the drop together, and it will break apart.

There have been numerous publications over the past 50 years on the evaporation and ion emission processes [15], [17]–[24]. While the droplets are larger than the Rayleigh radius for a given charge Q, the water evaporates until the droplet radius reaches the Rayleigh critical value at which point the drop sheds typically about 80% of its charge but only about 1% of its mass. Then, the process repeats itself. This has been observed directly in the experiments of Duft *et al.* [20].

The surface energy $U(r)$ of a droplet having charge Q comprises the usual surface tension term and a repulsive term due to the excess charge. Thus, [21]

$$U(r) = 4\pi r^2 \gamma + Q^2/8\pi\varepsilon_o r.$$

Rayleigh's limit earlier arose from a perturbation analysis of the stability of a sphere drop subject to the net radial force $\partial U/\partial r$.

Ichiki and Consta [22] have performed molecular dynamics simulations of nanodroplet disintegration finding that, by far, the most common scenario was that the fragment splitting off comprised a single ion with several solvent molecules.

At some point, the binding energy sodium and chloride ions together will overcome the hydrating ability of the water in the droplet. At room temperature, salt crystals would be precipitated out much as one finds near the sea [8]–[10]. At high temperatures, however, the sodium chloride will simply be dissociated

$$\mathrm{NaCl(aq)} \rightarrow \mathrm{NaCl(s)} \rightarrow \mathrm{NaCl(g)} \rightarrow \mathrm{N(g)} + \mathrm{Cl(g)}.$$

This will be discussed further as follows in the section on plasma chemistry.

At the high temperatures, above about 1500 °C, in the vicinity of the electrode tip, the micrometer-size saltwater droplets will evaporate very quickly on a timescale of a submillisecond. Any hydrated sodium and chorine ionic cluster, $\mathrm{Na}^+ \bullet (\mathrm{H_2O})_n$ and $\mathrm{Cl}^- \bullet (\mathrm{H_2O})_m$, will subsequently dissociate into $\mathrm{H_2O}$ molecules and atomic ions. The hydrated ion equilibrium will be discussed in detail as follows.

As Frost [25] has shown, if the heating of the drops is very rapid, explosive boiling of the droplets may occur. Whether the water in the saltwater drop evaporates away in a stable manner, as is expected at room temperature, or explosively has no effect upon this discussion, a large number of Na^+ and Cl^- ions and hydrated clusters will be released into the local environment in addition to $\mathrm{H_2O(g)}$, Na(g), and Cl(g) species.

We expect the composition of the plasma near the needle to be Na^+ and Cl^- ions, ions and radicals of the $\mathrm{N_2}$ and $\mathrm{O_2}$ that comprise air, $\mathrm{H_2O}$ molecules, and ions and radicals arising from the breakup of $\mathrm{H_2O}$. The electrons from the thermionic emission and collisional ionization processes should be rapidly lost to attachment and recombination. The plasma above the needle is known as a recombining plasma or an afterglow. As we will discuss as follows, this plasma chemistry is exothermic.

IV. Structure and Plasma Chemistry of the Flame

A. Temperature Profiles

Although the flow rate is 240 cm/s, the timescale for the plasma chemistry is much shorter than the hydrodynamic timescale. A reasonable assumption then, given the disparity in timescales, is that the plasma is always in local thermodynamic equilibrium at the local temperature. Equilibrium speciation calculations of the composition of high-temperature air have been pursued for decades. Hence, we can draw on this prior work in our modeling of the plasma chemistry of this experiment.

We have already noted that the temperature of the tip of the electrode is near the 5555-°C vaporization temperature of the tungsten. The plasma sphere around the tip, which is 1–2 cm in diameter, is then in the thousands of degrees Celsius. The temperature a few centimeters away from the tip is about that of the air in the room. From the work of Zinn and Sutherland [26], we expect the composition of the plasma to be $\mathrm{N_2}$, O, H, OH, e^-, NO^+, Na^+, Na, Cl, and a variety of electronically excited atoms and molecules. Among the last, we expect large concentrations of $\mathrm{Na}(3^2P)$ and the metastable oxygen species $\mathrm{O}(^1D)$ and $\mathrm{O_2}(a^1\Delta)$. The ultraviolet radiation from the hot electrode tip will have photodetached any negative ions. Most of the sodium ions are from the excess ions ejected from the charged saltwater droplets. The solid NaCl(s) residue after evaporation of the water from the drops will be dissociated into Na(g) and Cl(g) but, based on the work by Zinn and Sutherland and estimates made using Saha's equation, should not be highly ionized. The presence of free chlorine is apparent from the growth of tungsten pentachloride $(\mathrm{WCl_5})$ crystals, as seen in Fig. 2, on the cooler region of the tungsten needle below the hot tip.

Fig. 2. Ten times microphotograph of $\mathrm{WCl_5}$ crystals deposited near the tip.

As the plasma cools in the flame region above the electrode, the free electrons in the absence of a driving E-field rapidly disappear via recombination or attachment of the most obvious reactions being

$$e^- + \mathrm{NO}^+ \rightarrow \mathrm{N} + \mathrm{O}$$

$$e^- + \{\mathrm{Cl}, \mathrm{NO}, \mathrm{OH}\} \rightarrow \mathrm{Cl}^-, \mathrm{NO}^-, \mathrm{OH}^-.$$

As sodium has the smallest ionization potential of any species in the plasma, charge transfer from other positive ions will make Na^+ the dominant positive atomic ion. Similarly, atomic chlorine has the largest electron affinity and hence will, via charge transfer, become the dominant negative atomic ion. Recombination and neutralization of positive and negative ions in a plasma are generally very fast processes. For Na^+ and Cl^-, the following reactions are generally invoked:

$$\mathrm{Na}^+ + \mathrm{Cl}^- \rightarrow \mathrm{Na} + \mathrm{Cl}$$

$$\mathrm{Na}^+ + \mathrm{Cl}^- + M \rightarrow \{\mathrm{NaCl \text{ or } Na} + \mathrm{Cl}\} + M.$$

The neutralization process in the first reaction has a finite rate even as the pressure goes to zero. The rate of the second reaction increases linearly with pressure at subatmospheric gas densities and then decreases at higher pressure because it becomes diffusion limited.

Whitten *et al.* [27] investigated these reactions in detail 30 years ago with regard to the sodium chloride chemistry in flames at atmospheric pressure near 2000 °C. Their conclusion was that Na + Cl, i.e., the neutralization channel, were the dominant products.

Because the RF fields interfered with our thermocouple probes, we were not able to measure the temperature profile $T(z)$ vertically above the electrode and plasma sphere. Measurements performed with the same configuration using a

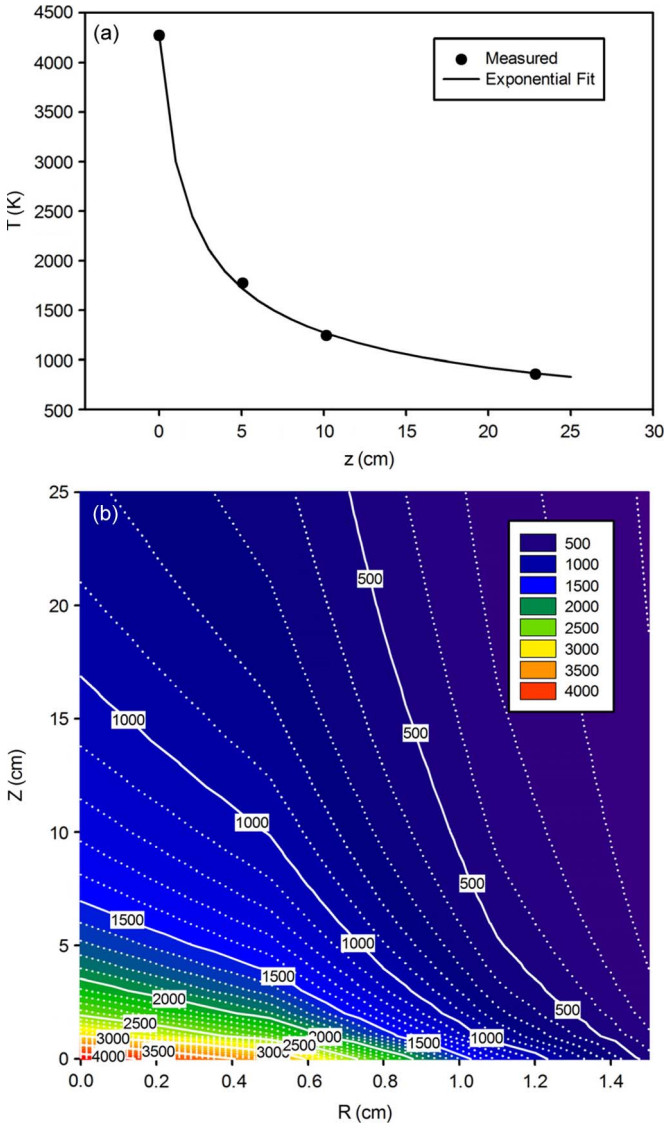

Fig. 3. (a) Vertical temperature profile at the center of a flame produced by a conventional ac arc. (b) Model temperature contours $T(r, z)$ using the vertical temperature profile of this figure and a Gaussian radial profile.

conventional two-electrode ac arc showed temperatures as high as 300 °C 30 cm above the arc plasma. The measured axial $T(z)$ profile from those experiments is shown in Fig. 3(a). We expect the vertical temperature profile in this experiment to be similar.

Based on our arc measurements, we expect the temperature a centimeter or two above the plasma sphere to be down to, perhaps, 1500 °C–2000 °C. This is the starting point for our model calculations. There have been many hundreds of research articles published in the past century on the physics and plasma chemistry in the high-temperature plasma region of arcs [28], [29]. We will concern ourselves here with the flowing afterglow region.

Fig. 3(b) shows a diagram illustrating the various regions of the plasma and flame. Above the 1–2-cm-diameter plasma sphere surrounding the tungsten needle tip, the plasma is approximately cylindrical extending vertically some 30 cm or more. The plasma core is, as we have noted, some 4000 °C slightly above the electrode falling to several hundred degrees 30+ cm higher. The plasma comprises the hot core surrounded by a cooler intermediate region and an outer transition region that eventually blends into the ambient room temperature air.

B. Plasma Chemistry

Our conceptual model of this plasma structure and chemistry is similar to that proposed by Turner [30] for ball lightning. We will discuss later how the model that we develop here may also be applicable to the recent experimental research on so-called plasmoids and other similar phenomena.

A number of authors over the years have studied the equilibrium chemistry of high-temperature air. The most well known is, arguably, the work of Gilmore [31], [32] at Rand Corporation in the 1950s and 1960s. We have used Gilmore's results and the more recent work of Zinn and Sutherland [26] as a starting point in our model of the afterglow physics and chemistry.

A moderately complete set of reactions comprising the sodium and chlorine plasma chemistry at temperatures of $T >$ 1500 °C might be

$$\mathrm{Na^+ + Cl^- \rightarrow \{NaCl, Na + Cl\}}$$
$$\mathrm{Na^+ + Na} + M \rightarrow \mathrm{Na_2{}^+} + M$$
$$\mathrm{Na_2{}^+ + Cl^- \rightarrow NaCl + \{Na, Na^*\}}$$
$$\mathrm{Na + Cl_2 \rightarrow NaCl + Cl}$$
$$\mathrm{Cl + Na_2 \rightarrow NaCl + Na^*}$$
$$\mathrm{Na^* + N_2 \rightarrow Na + N_2}$$
$$\mathrm{Na^* + Na^* \rightarrow Na_2{}^+} + e^-$$
$$\mathrm{Na^* + Na} + M \rightarrow \mathrm{Na_2{}^*} + M$$
$$\mathrm{Na^* \rightarrow Na} + h\nu \ (\lambda = 589 \text{ nm})$$
$$\mathrm{Na_2{}^* \rightarrow 2\ Na} + h\nu \ (\lambda = 500{-}800 \text{ nm})$$

Recall that, due to the preponderance of water drops in the flow entering the hot region around the electrode, the plasma above the electrode is likely to consist mostly of H_2O molecules and fragments in a much greater concentration than the ∼2% that is found in saturated air at room temperature. There will obviously be some N_2 and O_2 and their high-temperature reaction products and fragments as well.

Using an optical spectroscope and a digital camera, we were able to measure the emission spectrum shown in Fig. 4. The sodium 589-nm emission is apparent. We have also graphed in Fig. 4 the 6000-K blackbody spectrum and a typical spectrum of a sodium lamp showing the sodium dimer emission. Because the dimer emission peaks in the same wavelength region as does the 6000-K emission, it would be very difficult in an experiment such as this one to assess from their emission the relative concentration of sodium dimers. That the continuous portion of the spectrum peaks in the same spectral region as the 6000-K emission is consistent with our observation that the tip of the tungsten needle is near the 5555-°C tungsten vaporization temperature.

As the temperature falls below ∼1500 °C, sodium clusters will begin to form: $\mathrm{Na^+ \bullet (H_2O)}_n$, $\mathrm{Na \bullet (H_2O)}_n$, and $\mathrm{Na^* \bullet (H_2O)}_n$. Bates and Morgan [33], [34] have shown that cluster ions tend to have very large ion–ion recombination rates, due to tidal effects. It is very well known, however, that the sodium in the $\mathrm{Na^+ \bullet (H_2O)}_n$ cluster ion lies in the interior of the cluster. The negative cluster ion $\mathrm{Cl^- \bullet (H_2O)}_m$, on the other hand, has the Cl^- on the anterior of the cluster [35]. Shevkunov [36]

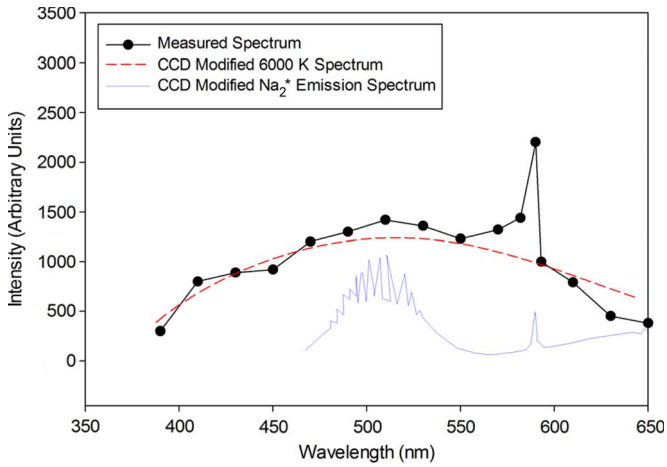

Fig. 4. Measured flame spectrum, 5800-K blackbody spectrum modified by the CCD response, and a published Na_2^* emission spectrum modified by the CCD response.

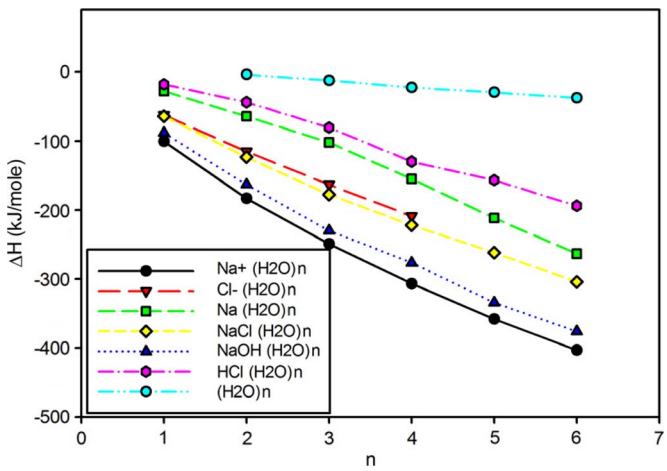

Fig. 5. Hydration enthalpies of molecular clusters that may be found in the regions of the flame.

has shown that, due to the topology of the clusters, the ionic recombination rate is very slow. A cluster of the form $Cl^- \bullet (H_2O)_m \bullet Na^+ \bullet (H_2O)_n$, i.e., a solvent-separated ion pair [36], can only become a contact ion pair (CIP) by ionic diffusion in the hydrated cluster, which is a slow process.

Hydrated Cl^- clusters are easily photodetached. As the neutral cluster is very weakly bound [37]–[39], it tends to dissociate.

We expect in the cooler regions of the plasma having $T > 500$ °C, for example, a large concentration of hydrated sodium clusters of the form $Na \bullet (H_2O)_n$. These have photoabsorption cross sections $\sigma \simeq 10^{-16}$ cm^2 over a broadband of wavelengths [40]. We anticipate that some of the Na^* and Na_2^* emissions in the hot core of the plasma column will be trapped by the hydrated sodium clusters

$$Na \bullet (H_2O)_n + h\nu \rightarrow Na^* \bullet (H_2O)_n.$$

In the cooler regions of the plasma, where the temperature is less than about 1000 °C, we expect the sodium atoms, NaCl, NaOH, and HCl molecules to be bound to water molecules in the form of hydrated clusters. Any free Na^+ and Cl^- ions would exist as $Na^+ \bullet (H_2O)_n$ and $Cl^- \bullet (H_2O)_m$ clusters. $n = 1$ is the most probable hydrated Na^+ cluster at $T \simeq 1200$ °C, and $m = 1$ is the most probable hydrated $Cl^- \bullet (H_2O)_m$ cluster at $T \simeq 700$ °C. As temperature decreases from these values, the sizes of the clusters increase.

Similarly, depending on the temperature, $Na \bullet (H_2O)_n$, $Na^+Cl^- \bullet (H_2O)_n$, $Na^+OH^- \bullet (H_2O)_n$, and $H^+Cl^- \bullet (H_2O)_n$ will be found in various hydration states and densities. Fig. 5 shows the enthalpies of hydration $\Delta H_{0,n}$ for clusters of up to six water molecules [41]–[50]. The enthalpies are with respect to the $n = 0$ value. The enthalpy $\Delta H_{0,n}$ is

$$\Delta H_{0,n} = \Sigma_{i=1}^{n} \Delta H_{i-1,i}$$

where $\Delta H_{i-1,i}$ is the incremental enthalpy change for the reaction

$$X \bullet (H_2O)_{i-1} + H_2O \Leftrightarrow X \bullet (H_2O)_i.$$

As the cluster size n becomes large

$$\Delta H_{n-1,n} \rightarrow \Delta H_{vap}(H_2O) \simeq 44 \text{ kJ/mol}$$

i.e., the enthalpy of vaporization of liquid water.

Just what the cluster sizes and densities are depends upon the equilibrium constants

$$K_{n-1,n}(T) = \exp[-\Delta G_{rxn}/RT]$$

where ΔG_{rxn} is Gibbs' free energy of reaction. Gibbs' free energy is related to the enthalpy and entropy by $G \equiv H - TS$. The temperature dependence of the equilibrium constants is given by van't Hoff's equation

$$\text{Ln}\left(\frac{K}{K_{\text{ref}}}\right) = -\left(\frac{\Delta H_{\text{rxn}}}{RT}\right)(T/T_{\text{ref}} - 1).$$

From Fig. 5, we see that the most strongly bound neutral clusters are those of NaOH, NaCl, and Na. As the value of n increases to values greater than about four to six, charge separation occurs in the clusters so that [51]–[53]

$$X^+Y^- \bullet (H_2O)_n \rightarrow X^+ \bullet (H_2O)_k \bullet Y^- \bullet (H_2O)_{n-k}.$$

That is, the molecule of electrolyte becomes dissolved with the charges separated by hydration shells. Ultimately, as the vapor cools, drops are formed containing not only dissolved NaCl but also NaOH and HCl.

Of particular interest to us are the clusters $Na \bullet (H_2O)_n$. For n in the range of four to ten, the charge separation leads to the following [51]–[53]:

$$Na \bullet (H_2O)_n \rightarrow Na^+ \bullet (H_2O)_n e^- \rightarrow Na^+OH^- \bullet (H_2O)_{n-1} + H$$

followed by further charge separation of the Na^+OH^-. Where $Na \bullet (H_2O)_n$ exists, the clusters possess absorption bands over the wavelength range 500 nm $\leq \lambda <$ 1400 nm having cross sections of about 10^{-16} cm^2 [40]. The cross sections for $1 \leq n \leq 8$ all have about the same value.

The $Na(H_2O)_n$ clusters will absorb the $Na(3^2P \rightarrow 3^2S)$ 589-nm resonance radiation emitted by the hot core of the plasma and re-emit and reabsorb and so on over the width of

the band. The net effect of this is to increase the opacity over what the gas would have if the sodium were tied up as NaCl(g) or hydrated clusters outside the hot core but leads to an opacity that is less than it would be if that subvolume of the gas were populated with atomic sodium.

Eventually, as the gas cools with distance above the RF electrode, the composition of the gas is N_2, O_2, $H_2O(v)$, and the usual N_xO_y products that arise from plasmas in air. There will be some NaO_x and ClO_x products [54], [55] as well. The zwitterionic clusters will continue to nucleate leading to droplets of finite size containing dissolved NaCl, NaOH, and HCl. We have observed these hydrated products in other plasma experiments involving saltwater aerosols and mists.

From the strong optical emission, mostly from sodium, shown in Fig. 1, we expect that to be a very important part of the plasma chemistry. Assuming the $Na(3^2P)$ excited state and $Na(3^2S)$ ground state to be in Boltzmann equilibrium at, for example, 2000 °C, the ratio of the populations will be

$$\frac{[Na^*]}{[Na]} = (g_{3P})/g_{3S}) \exp\left[-\Delta\varepsilon/kT\right] = 1.5 \times 10^{-5}$$

where $\Delta\varepsilon = 2.1$ eV.

Given the large density of sodium expected in the plasma from the 35 g/L of salt in the water, there will be a high density of excited sodium atoms. The number density should be on the order of $[Na^*] \simeq 10^{14}$ cm^{-3}.

Due to the absence of an external source of power, once the plasma is created at the needle tip and to the very rapid recombination rate, the hot gas should only be very weakly ionized above the tip. We expect Saha–Boltzmann equilibrium to be a good approximation in most of the flame. The flame will have a hot central core with $T(z)$ similar to that shown earlier. $T(r)$ will be a function having its maximum at $r = 0$ and approaching the ambient air temperature at some distance R from the center. Although the columnar flame is some 2 cm in radius and has a central temperature of several thousand degrees, the temperature is close to ambient at a radius of only 4–5 cm from the center. The situation here is very much like that found in arc discharges [28].

The primary candidates as the cooling mechanisms for the flame are heat conduction down the thermal gradient of $T(r)$ and radiation, both thermal, i.e., blackbody or gray body, and line or band radiation.

In the heat equation, the heat flux $\Gamma = \kappa\partial T/\partial r$ is written in the same form as the mass flux in the diffusion equation where $\kappa \equiv \lambda/\rho C_p$ is the thermal diffusivity. λ is the thermal conductivity, ρ is the density, and C_p is the specific heat. The units of Γ are watts per square centimeter. For example, in high-temperature air, $0.1 \leq \kappa \leq 0.5$ cm^2/s for 2000 K $\leq T \leq$ 4000 K. The thermal flux radially through the flame is less than $\Gamma \simeq 1$ W/cm^2. The energy density due to thermal motion is less than ~ 1 J/cm^3.

V. Radiative Power Loss

If we consider Planck blackbody emission from the hot gas we have available, the emissivities (in watts per cubic centimeter) and the opacities or absorption coefficients (in per centimeter) compiled by Gilmore [32] for high-temperature air. At 4000 K and atmospheric pressure, the emissivity is only $\sim$0.1 W/cm^3. The opacity integrated over the Planck spectrum is only 10^{-5}/cm at 4000 K. That is, thermal radiation is only a minor component in the power balance.

Given that significant components of the plasma are sodium, a group I metal, and its dimer and hydrated clusters, we expect line and band emission and absorption to be of importance. Line and band emission and, in particular, absorption and opacity issues are extremely complex. They have been an area of very intense research since the early 20th century and are critical to stellar and planetary atmospheres [56] and other systems, such as hot dense plasmas, that are dominated by radiation hydrodynamics. In this analysis, we will demonstrate that the opacity of the flame is such that we can treat the radiation transport as a diffusion problem thus simplifying our power balance estimates.

Atomic spectral lines have a natural width in frequency or wavelength as a consequence of Heisenberg's principle. This is only realized in observations under conditions of near-zero absolute temperature, near-zero ambient pressure, and in the absence of other perturbations such as electric or magnetic fields. Under the conditions found in a flame, the spectral lines are broadened primarily by two effects. At higher temperatures, the lines are broadened by Doppler effects due to the atomic thermal motion. At lower temperatures, they can be broadened by collisions within the plasma. The former line profile is known as the Doppler profile, which, not surprisingly, is a Gaussian function. The latter profile is the well-known Lorentz function and is wider in the wings than the Gaussian function.

If $\lambda_\nu(x)$ is the photon mean free path at location x, for frequency ν, the optical depth τ_ν is defined by

$$\tau_\nu = \int dx'/\lambda_\nu(x').$$

That is, it is the number of photon mean free paths along the path of length x. The reciprocal of the mean free path, i.e., $\alpha_\nu = \lambda_\nu^{-1}$, is known variously as the extinction coefficient, absorption coefficient, or opacity.

For resonance radiation, such as the 589-nm $Na(3^2P_{1/2,3/2} \rightarrow 3^2S_{1/2})$ doublet lines emitted by electronically excited sodium, line broadening determines how rapidly radiation escapes an optically thick, i.e., having great optical depth, plasma. The frequency-dependent absorption coefficient α_ν is much smaller in the line wings than it is at the line center. A photon emitted at line center, for example, may be readily reabsorbed in a short distance but then may be re-emitted out in the wing of the spectral line where it is less likely to be reabsorbed. The frequency redistribution eventually allows the photons to escape the medium. In very optically dense media, the high-pressure sodium lamp is an example; one can even observe line reversal where the radiated intensity near the line center is much less than that on either side of the line center.

The radiative lifetime of the sodium 3^2P excited state, lumping the $3^2P_{3/2}$ and $3^2P_{1/2}$ states together, at 589 nm or

2.1 eV is about 16 ns. Einstein's A-coefficient is then $A = 6.25 \times 10^7$ s^{-1}. Holstein [57], [58] has provided expressions for the optical depth and escape probabilities for Doppler (temperature) and Lorentz (pressure) broadened atomic emission lines. The Doppler optical depth is given by

$$\tau = \left(\frac{\lambda_0^3 N_0}{8\pi}\right)\left(\frac{g_u}{g_l}\right)\left(\frac{A}{v_0 \pi^{\frac{1}{2}}}\right) L$$

where λ_o is the wavelength; N_o is the population of the lower, i.e., Na($3^2S_{1/2}$), state; g_u and g_l are the statistical weights; L is distance into the medium, e.g., the thickness of a slab or radius of a cylinder; and $v_0 = (2kT/M)^{1/2}$ is the average thermal speed of the radiating atoms.

Holstein's expression for the escape probability is

$$P = \frac{\xi}{[\tau(\pi \ln(\tau) 1/2]}$$

when $\tau > 2.5$ and

$$P = e^{-\phi\tau}$$

when $\tau \leq 2.5$. ϕ is a normalization constant designed to make the two formulas equal at $\tau = 2.5$. As we are modeling the plasma as a cylindrical column, the geometrical factor $\xi = 1.6$ for cylindrical geometry.

The loss rate of the excited sodium Na* atoms due to radiative decay

$$\text{Na}^* \rightarrow \text{Na} + h\nu$$

is

$$\frac{d[\text{Na}^*]}{dt} = -PA\,[\text{Na}^*]$$

or

$$[\text{Na}^*] = [\text{Na}^*]_o \exp[-PAt].$$

The smaller the value of the escape probability, the longer the effective radiative lifetime is due to the radiation trapping.

Milne, in 1926 [59], provided the theory for transport of line radiation through a plane parallel slab, i.e., a mass of gas in $0 \leq x \leq L$. If, at any given time, there are N_0 atoms/cm^3 in the ground state and N^* atoms in an excited state, the N^* atoms can emit photons and the N_0 atoms can absorb the photons. The density at any given point x is given by

$$\frac{\partial^2}{\partial x^2 (N^* + \tau \partial N^*/\partial t)} = \frac{4\alpha^2 \tau \partial N^*}{\partial t}$$

where $\tau = A^{-1}$ is the radiative lifetime and α is the absorption coefficient. The forward $(+)$ and backward $(-)$ radiation fluxes are given by

$$\pi I_{\pm} = \left(\frac{\pi\sigma}{N_0}\right)\left[\frac{F^*(x,t)(-1)^{\pm 1}(Z\alpha)^{-1}\partial F^*(x,t)}{\partial x}\right]$$

where $F^*(x,t) = N^* + \tau \partial N^* Z/\partial t$. The constant σ is defined by

$$\sigma \equiv \left(\frac{g_0}{g_2}\right)\left(\frac{2h\nu^3}{c^2}\right).$$

Milne obtained a series solution for πI_+ in terms of factors $\exp(-\beta_i t)$.

The effective A-coefficient is given by

$$\beta = \frac{A}{\left[1 + \left(\frac{\alpha L}{\lambda}\right)^2\right]}$$

where $\lambda \simeq \pi/2$ is the first root of the transcendental equation

$$\lambda \tan(\lambda) = \tau.$$

Thus, the effective radiative lifetime is

$$\tau_{\text{eff}} = \beta^{-1} = \tau\left[1 + \left(\frac{\alpha L}{\lambda}\right)^2\right].$$

Bilckensderfer *et al.* [60] have applied Milne's approach to a gas having cylindrical symmetry. The solution for $N^*(r,t)$ is a Bessel function series, as one typically finds for solutions to the diffusion equation in cylinders (refs)

$$N^*(r,t) = \Sigma_m A_m J_o(\lambda_m r) \exp(-t/\tau_m)$$

where the λ_m denotes the roots of the transcendental equation

$$\lambda_m R J_1(\lambda_m R) = Z\alpha R J_o(\lambda_m R).$$

The decay times in the expansion are

$$\tau_m = Z\left[1 + 4\left(\frac{\alpha}{\lambda_m}\right)^2\right]$$

which is much like the expression for the decay times in the slab geometry.

Samson [61] and Kenty [62] had made use of an "effective" opacity $\langle\alpha\rangle L$ in order to formulate the radiation transfer problem in terms of a diffusion coefficient.

Holstein [57] has shown that the diffusion model using an effective opacity or mean free path provides an inaccurate description for large opacities, but he nevertheless states that this approach yields results that are in fair agreement with the more exact theory and with experiment. We will use this approach in estimating the effective radiative lifetime of the Na(3^2P) states and, hence, the energy balance of the plasma.

Given the prescribed Gaussian model temperature profile across the flame, which we introduced earlier, we subdivided the r-axis into numerous bins of width Δr taking [Na($3s$)] and T to be constant across each bin. The effective Na(3^2P) lifetime was calculated to be 0.11 s, which is very close to the $\sim$1/8-s sodium emission time from the flame.

Considering only the central core of the flame with $N^*(t) = N^*(t=0)\exp(-t/\tau_{\text{eff}})$, we can estimate $T(z) = v_z \partial T/\partial t$ up

the flame column due to loss of resonance radiation. The power balance equation is

$$\frac{\rho C_p \partial T}{\partial t} = -P_{\rm rad}(t)$$

where $P_{\rm rad}(t) = \Delta\varepsilon_{3p3s}\partial N^*(t)/\partial t$. From the values that we presented earlier, the energy density at $T(r=0, t=0) = 4000$ K is about 4123 J/cm^3. When the gas is transparent to the 589-nm radiation, the Na(3^2P) states would decay away in less than a microsecond. Using this trapping model, the temperature drops the rate of 812 K/s. That this loss rate is far too small, i.e., the opacity in the model is too large, indicates that a much better 2-D model incorporating not only the line transfer but also the band transfer with more accurate calculations of all the molecular species and hydrated clusters is required.

VI. Summary of Flame Study

The flame rising in the region above the high-temperature plasma surrounding the ~1-kW RF needle is a very weakly ionized hot gas that may be considered to be the afterglow of the driven plasma near the needle antenna. The primary constituents of the hot core of the flame are Na, Na^*, Cl, H_2O, N_2, O_2, and some NO_x. Due to the high sodium densities, the gas is optically thick to the 589-nm Na$(3^2P \rightarrow 3^2S)$ resonance radiation from the core region. This radiation trapping increases the effective lifetime of Na^* from 16 ns to tens to hundreds of microseconds. The radiation eventually diffuses out of the gas through the wings of the spectral line.

Some sodium dimers, Na_2, exist in the hot gas. These can absorb the Na^* resonance radiation and re-emit in bands on either side of the 589-nm line.

In the cooler regions of the flame, the Na and Cl are taken up into hydrated clusters $Na \bullet (H_2O)_n$ and $Cl \bullet (H_2O)_m$. Eventually, CIPs such as $Na^+Cl^- \bullet (H_2O)_n$ form $Na^+ \bullet (H_2O)_n \bullet Cl^- \bullet (H_2O)_m$, where the sodium and chloride ions are solvated and become the nuclei for further condensation to form liquid drops. Hydrated clusters of NaOH and HCl are similarly formed. The hydrated sodium atoms can absorb Na^* and Na_2^* radiation and reradiate in bands in the near IR.

In short, the extended flame is a result of the high density of sodium and the strong radiation trapping, much as in a sodium lamp [63]. This amounts to being an open-air single-electrode sodium lamp using saltwater rather than sodium vapor.

VII. Other Recent Research on Water Plasmas

Electric discharges involving water have been the subject of research for well over a century, perhaps even two centuries. Whereas we are reporting here upon plasma formation in a saltwater spray, our previous work [1], [64] involved a very short pulse high-energy-deposition discharge in a liquid saltwater solution.

There have been other experiments and analyses, both older and much more recent, that may have some relevance to our work.

In 1986, Radovanov *et al.* [65], [66] published experiments and plasma composition modeling for pulsed discharges in $H_2O/NaNO_3$ solutions. These were high-current high-energy-deposition tens-of-microseconds pulsed discharges.

There has long been a discussion in the scientific literature about the role that gas bubbles may play in the initiation and propagation of electric discharges in liquid water. Whereas we have discussed herein a plasma in spray containing a high density of micrometer-size water droplets, a recent trend has been to study plasmas in liquid water containing bubbles [67].

Some of the recent work [68], [69] has been on discharges within gas bubbles in liquids showing that the preferred discharge channel is along the interface between the gas and the liquid rather than across the bubble.

Although the general consensus has been that gas bubbles play a significant role in discharges in liquids, recent work by Starikovskiy *et al.* [67] appears to show that, for very short pulses, bubbles in the water are unnecessary.

In yet another very recent study of discharges in water vapor, which lies between the two extremes discussed earlier, Skoro *et al.* [70] have plotted out a complete Paschen curve over a wide range of pd, pressure times electrode gap.

VIII. Extension of the Model to Other Experiments

A. Plasmoids

The authors of [71]–[75] describe experiments involving millisecond high-voltage and high-current discharges through aqueous electrolyte solutions and the creation there from the long-lived structures known as "plasmoids." Plasmoids are globules of glowing plasma in the air above the liquid that persist for tens to hundreds of milliseconds.

The photographs in Fig. 6 show a similar but shorter lived phenomenon in an experiment of ours. Experiments such as this one are easy to implement. There are scores of videos of saltwater explosions posted on the Internet by amateur experimenters. Our experiment involved discharging a 450-μF capacitor charged to 2200 V across a 0.5-cm gap between the tips of small tungsten electrodes lying in a groove on an alumina surface. The volume of saturated saltwater was only about 10 μL. Only a small fraction of capacitor charge was discharged through the salt solution. The fireball is about 15 cm across at 8–10 ms after the discharge ignition (Fig. 6).

The plasmoid experiments involve a larger volume of water and a more symmetric discharge than did our simple experiment and are likely, because of this, longer lived. The plasma chemistry is likely very similar to that of our RF-produced flame. The most significant features of the physics and plasma chemistry involving trapped line radiation and hydrated clusters are, no doubt, common to both experiments and result in similar behavior.

B. RF Experiments of Roy and Kanzius

Roy *et al.* [76], [77] have described experiments in which a test tube of saltwater irradiated by 600 W of 13.56-MHz RF radiation emits a flame similar to but much smaller than the one we observed in our experiments. We propose that the flame

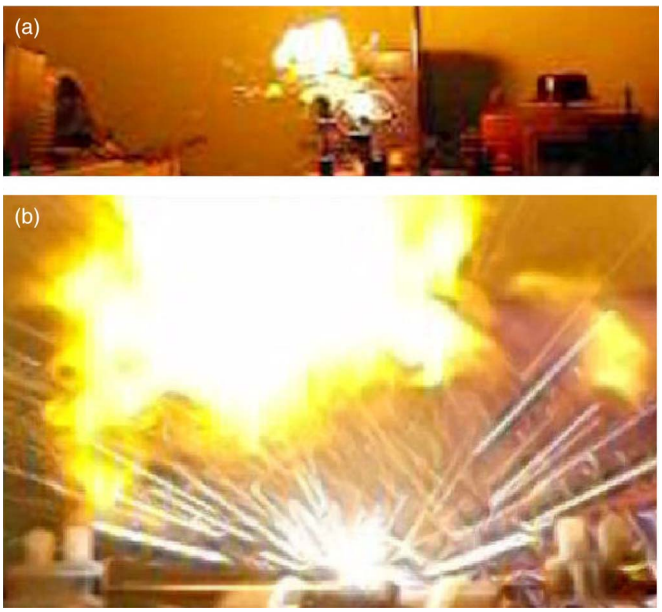

Fig. 6. Fireball and 589-nm sodium emission on the millisecond timescale from videos of an open-air saltwater discharge: (a) 1000 and (b) 420 ft/s.

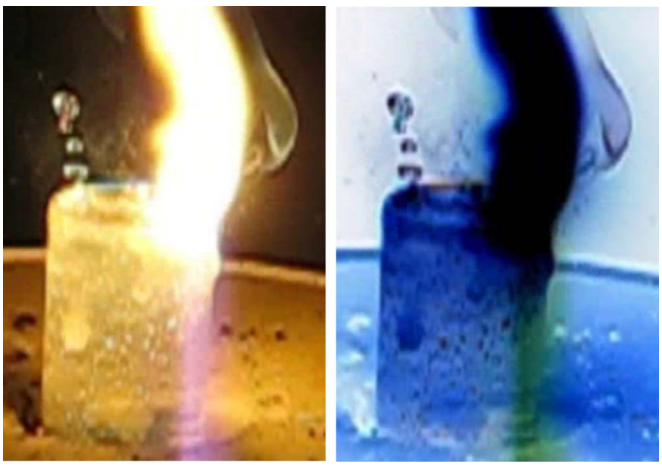

Fig. 7. Rising air bubbles and saltwater drops created at the water–air interface in a test tube of saltwater irradiated by ∼1 kW of 13.56-MHz RF waves; the rising bubbles are more easily seen in the negative image.

mechanism in their experiments is much like that described herein.

As can be seen in the photographs [76] of Roy *et al.* experiments, the RF irradiation heats the saltwater to near boiling leading to a large flux of macroscopic bubbles rising to the surface. These can be seen in Fig. 7 taken during one of our RF + liquid saltwater experiments using the RF antenna configuration of Roy *et al.* [76]. Blanchard [8]–[10] has shown that, in seawater, such bubbles produce numerous saltwater drops and free ions when they reach the surface.

From that point, the strong RF electric field may produce a plasma in the boundary region above the water in the test tube. In our experiments, the only external driving force was the tungsten electrode itself. In the Roy *et al.* [76] experiments, the flame continues to be driven by the RF field as the test tube and flame lie between the RF antennas. This is very much like the small flame from a candle or match in a microwave oven being driven by the 2.45-GHz E-field in the resonant microwave cavity of the oven. This is an experiment that many scientifically inclined owners of microwave ovens have performed in their kitchens!

ACKNOWLEDGMENT

The authors would like to thank B. Clark for his aid in these experiments. The authors dedicate this paper to the late J. Kanzius and the late Prof. R. Roy as it was their work that stimulated the authors in 2007 to undertake their research on saltwater discharges and plasmas.

REFERENCES

[1] W. L. Morgan and L. A. Rosocha, "Surface electrical discharges and plasma formation on electrolyte solutions," *Chem. Phys.*, vol. 398, pp. 255–261, Apr. 2012.
[2] I. E. Kieft, E. P. v d Laan, and E. Stoffels, "Electrical and optical characterization of the plasma needle," *New. J. Phys.*, vol. 6, pp. 149-1–149-14, 2004.
[3] S. Lazović, N. Puac, G. Malović, A. Dordević, and Z. L. Petrović, "Diagnostic of plasma needle properties by using mass spectrometry," *Plasma Sources Sci. Technol.*, vol. 19, pp. 034014-1–034014-7, 2010.
[4] C. Rodes, T. Smith, R. Crouse, and G. Ramachandran, "Measurements of the size distribution of aerosols produced by ultrasonic humidification," *Aerosol Sci. Technol.*, vol. 13, no. 2, pp. 220–229, 1990.
[5] J. Zeleny, "The electrical discharge from liquid points, and a hydrostatic method of measuring the electric intensity at their surfaces," *Phys. Rev.*, vol. 3, no. 2, pp. 69–91, Feb. 1914.
[6] J. Zeleny, "Electrical discharges from pointed conductors," *Phys. Rev.*, vol. 16, no. 2, pp. 102–125, Aug. 1920.
[7] W. N. English, "Corona from a water drop," *Phys. Rev.*, vol. 74, no. 2, pp. 179–196, Jul. 1948.
[8] D. C. Blanchard, "Electrically charged drops from bubbles in sea water and their meteorological significance," *J. Meteorol.*, vol. 15, no. 4, pp. 383–395, Aug. 1958.
[9] D. C. Blanchard, "The electrification of the atmosphere by particles from bubbles in the sea," *Prog. Oceanogr.*, vol. 1, pp. 71–202, 1963.
[10] D. C. Blanchard, "Positive space charge from the sea," *J. Atmos. Sci.*, vol. 23, no. 5, pp. 507–515, Sep. 1966.
[11] V. Schroeder, M. B. Baker, and J. Latham, "A model study of corona emission from hydrometeors," *Quart. J. R. Meteorol. Soc.*, vol. 125, pp. 1681–1693, 1998.
[12] A. A. Sinkevich, J. A. Dovgaluk, V. D. Stepanenko, and L. V. Kashleva, "Corona discharge in clouds (overview)," in *Proc. XII Int. Conf. Atmos. Elect.*, 2003, pp. 241–244.
[13] M. P. Boussaton, S. Colquillat, and S. Chauzy, "Influence of water conductivity on microdischarges from raindrops in strong electric fields," *Atmos. Res.*, vol. 76, no. 1–4, pp. 330–345, Jul./Aug. 2005.
[14] E. E. Dodd, "The statistics of liquid spray and dust electrification by the Hopper and Laby method," *J. Appl. Phys.*, vol. 24, no. 1, pp. 73–80, Jan. 1953.
[15] J. V. Iribarne and B. A. Thomson, "On the evaporation of small ions from charged droplets," *J. Chem. Phys.*, vol. 64, no. 6, pp. 2287–2294, Mar. 15, 1976.
[16] S. G. Brush and C. J. Wensrich, "Annotated bibliography of theories of the equation of state of ionized gases and strong electrolyte solutions," Univ. California, Bakersfield, CA, UCRL-6473, Aug. 8, 1961.
[17] D. G. Roth and A. J. Kelly, "Analysis of the disruption of evaporating charged droplets," *IEEE Trans. Ind. Appl.*, vol. IA-19, no. 5, pp. 771–775, Sep./Oct. 1983.
[18] H. M. A. Elghazaly and G. S. P. Castle, "Analysis of the instability of evaporating charged liquid drops," *IEEE Trans. Ind. Appl.*, vol. IA-22, no. 5, pp. 892–896, Sep./Oct. 1986.
[19] S. E. Law, "Charge and mass flux in the radial electric field of an evaporating charged water droplet: An experimental analysis," *IEEE Trans. Ind. Appl.*, vol. 25, no. 6, pp. 1081–1087, Nov./Dec. 1989.
[20] D. Duft, H. Lebius, B. A. Huber, C. Guet, and T. Leisner, "Shape oscillations and stability of charged microdroplets," *Phy. Rev. Lett.*, vol. 89, no. 8, pp. 084503-1–084503-4, Aug. 19, 2002.

[21] J. S. Shrimpton, "Dielectric charged drop break-up at sub-Rayleigh limit conditions," *IEEE Trans. Dielect. Elect. Insul.*, vol. 12, no. 3, pp. 573–578, Jun. 2005.
[22] K. Ichiki and S. Consta, "Disintegration mechanisms of charged aqueous nanodroplets studied by simulations and analytical models," *J. Phys. Chem. B*, vol. 110, no. 39, pp. 19 168–19 175, Oct. 2006.
[23] S. Nguyen and J. B. Fenn, "Gas phase ions of solute species from charged droplets of solutions," *Proc. Nat. Acad. Sci.*, vol. 104, no. 4, pp. 1111–1117, Jan. 23, 2007.
[24] C. J. Hogan, Jr., P. Biswas, and D. Chen, "Charged droplet dynamics in the submicrometer size range," *J. Phys. Chem. B*, vol. 113, no. 4, pp. 970–976, Jan. 2009.
[25] D. L. Frost, "Dynamics of explosive boiling of a droplet," *Phys. Fluids*, vol. 31, no. 9, pp. 2554–2561, Sep. 1988.
[26] J. Zinn and C. D. Sutherland, "Chemical equilibrium in hot air with moisture, salt, and vaporized metal contaminants," Los Alamos Scientific Lab, Los Alamos, NM, Los Alamos Rep. LA-5850-MS, Feb. 1975.
[27] B. L. Whitten, W. L. Morgan, and J. N. Bardsley, "Monte Carlo calculations of two-and three body ionic recombination," *J. Phys. B*, vol. 15, no. 2, pp. 319–326, Jan. 1982.
[28] Y. P. Raizer, *Gas Discharge Physics*. Berlin, Germany: Springer-Verlag, 1991.
[29] A. Fridman, *Plasma Chemistry*. New York: Cambridge Univ. Press, 2008.
[30] D. J. Turner, "The structure and stability of ball lightning," *Philos. Trans. Roy. Soc. London A, Math. Phys. Sci.*, vol. 347, no. 1682, pp. 83–111, Apr. 1994.
[31] F. R. Gilmore, "Equilibrium composition and thermodynamic properties of air to 24 000 °K," RAND Corp., Santa Monica, CA, RAND Corp. Rep. RM-1543, Aug. 1955.
[32] F. R. Gilmore, "Approximate radiation properties of air between 2000 and 8000 °K," RAND Corp., Santa Monica, CA, RAND Corp. Rep. RM-3997-ARPA, Mar. 1964.
[33] D. R. Bates and W. L. Morgan, "New recombination mechanism: Tidal termolecular ionic recombination," *Phys. Rev. Lett.*, vol. 64, no. 19, pp. 2258–2260, May 7, 1990.
[34] W. L. Morgan and D. R. Bates, "Tidal termolecular ionic recombination," *J. Phys. B, At. Mol. Opt. Phys.*, vol. 25, no. 24, pp. 5421–5430, Dec. 1992.
[35] O. Cheshnovsky, R. Giniger, G. Markovich, G. Makov, A. Nitzan, and J. Jortner, "Surface and interior anion solvation in water clusters," *J. Chem. Phys.*, vol. 92, no. 2, pp. 397–408, 1995.
[36] S. V. Shevkunov, "Ionization–recombination equilibrium in cold cluster plasma under conditions of retardation by high energy barrier," *High Energy Chem.*, vol. 42, no. 3, pp. 205–210, May 2008.
[37] M. Roeselova', G. Jacoby, U. Koldor, and P. Jungwirth, "Relaxation of chlorine anions solvated in small water clusters upon electron photodetachment. The three lowest potential energy surfaces of the neutral Cl^* • • • H_2O complex," *Chem. Phys. Lett.*, vol. 293, no. 3/4, pp. 309–316, Aug. 28, 1998.
[38] M. Roeselova', U. Koldor, and P. Jungwirth, "Ultrafast dynamics of chlorine-water and bromine-water and radical complexes following electron photo detachment in their anionic precursors," *J. Phys. Chem. A*, vol. 104, pp. 6523–6531, 2000.
[39] M. Roeselova', M. Mucha, B. Schmidt, and P. Jungwirth, "Quantum dynamics and spectroscopy of electron photodetachment in Cl^- • • • H_2O and Cl^- • • • D_2O complexes," *J. Phys. Chem. A*, vol. 106, no. 51, pp. 12 229–12 241, 2002.
[40] C. P. Schulz, C. Bobbert, T. Shimosato, K. Daigoku, N. Miura, and K. Hashimoto, "Electronically excited states of sodium-water-clusters," *J. Chem. Phys.*, vol. 119, no. 22, pp. 11 620–11 629, Dec. 2003.
[41] I. Dzidic' and P. Kebarle, "Hydration of the alkali ions in the gas phase—Enthalpies and entropies of reactions $M^+(H_2O)_{n-1} + H_2O = M^+(H_2O)_n$," *J. Phys. Chem.*, vol. 74, no. 7, pp. 1466–1474, Apr. 2, 1970.
[42] M. Arshadi, R. Yamdagni, and P. Kebarle, "Hydration of halide negative ions in the gas phase II. Comparison of hydration energies for the alkali positive and halide negative ions," *J. Phys. Chem.*, vol. 74, no. 7, pp. 1475–1482, Apr. 2, 1970.
[43] M. Meot-Ner and C. V. Speller, "Filling of solvent shells about ions. 1. Thermo chemical criteria and the effects of isomeric clusters," *J. Phys. Chem.*, vol. 90, no. 25, pp. 6616–6624, Dec. 1986.
[44] C. P. Schultz, R. Haugstatter, H.-U. Tittes, and I. V. Hertel, "Free sodium-water clusters: Photo ionization studies in a pulsed molecular beam source," *Z. Phys. D, At. Mol. Clusters*, vol. 10, no. 2, pp. 279–290, 1988.
[45] R. N. Barnett and U. Landman, "Hydration of sodium in water clusters," *Phys. Rev. Lett.*, vol. 70, no. 12, pp. 1775–1778, Mar. 22, 1993.
[46] L. M. Ramaniah, M. Bernasconi, and M. Parrinello, "Density-functional study of sodium in water clusters," *J. Chem. Phys.*, vol. 109, no. 16, pp. 6839–6843, Oct. 22, 1998.
[47] C. P. Petersen and M. S. Gordon, "Solvation of sodium chloride: An effective fragment study of $NaCl(H_2O)_n$," *J. Phys. Chem. A*, vol. 103, no. 21, pp. 4162–4166, May 1999.
[48] S. Odde, B. J. Mhin, S. Lee, H. M. Lee, and K. S. Kim, "Dissociation chemistry of hydrogen halides in water," *J. Chem. Phys.*, vol. 120, no. 20, pp. 9524–9535, May 22, 2004.
[49] A. Kumar, M. Park, J. Y. Huh, H. M. Lee, and K. S. Kim, "Hydration phenomena of sodium and potassium hydroxides by water molecules," *J. Phys. Chem. A*, vol. 110, no. 45, pp. 12 484–12 493, Nov. 2006.
[50] A. C. Olleta, H. M. Lee, and K. S. Kim, "Ab initio study of hydrated sodium halides $NaX(H_2O)_{1-6}$ (X = F, Cl, Br, and I)," *J. Chem. Phys.*, vol. 124, no. 2, p. 024321, Jan. 2006.
[51] K. W. Chan, C.-K. Siu, S. Y. Wong, and Z.-F. Liw, "The elimination of a hydrogen atom in $Na(H_2O)_n$," *J. Chem. Phys.*, vol. 123, no. 12, pp. 124 313-1–124 313-7, Sep. 2005.
[52] S. V. Shevkunov, "Charge separation in $Na^+Cl^-(H_2O)_n$ clusters in water vapors. 2. Free energy," *Colloid J.*, vol. 72, no. 1, pp. 107–124, 2010.
[53] S. V. Shevkunov, "Nucleation of water vapor on Na^+Cl^- ion pairs: Computer simulations," *Colloid J.*, vol. 73, no. 1, pp. 135–145, 2011.
[54] R. T. Watson, "Rate constants for reactions of ClO_x of atmospheric interest," *J. Phys. Chem. Ref. Data*, vol. 6, no. 3, pp. 871–917, 1977.
[55] A. J. Hynes, M. Steinberg, and K. Schofield, "The chemical kinetics and thermodynamics of sodium species in oxygen-rich hydrogen flames," *J. Chem. Phys.*, vol. 80, no. 6, pp. 2585–2597, Mar. 15, 1984.
[56] D. Mihalas, *Stellar Atmospheres*. San Fransisco, CA: Freeman, 1978.
[57] T. Holstein, "Imprisonment of resonance radiation in gases," *Phys. Rev.*, vol. 72, no. 12, pp. 1212–1233, Dec. 15, 1947.
[58] T. Holstein, "Imprisonment of resonance radiation in gases II," *Phys. Rev.*, vol. 83, no. 6, pp. 1159–1168, Sep. 15, 1951.
[59] A. C. G. Mitchell and M. W. Zemansky, *Resonance Radiation and Excited Atoms*. London, U.K.: Cambridge Univ. Press, 1971.
[60] R. P. Bilkensderfer, W. H. Breckenridge, and J. Simmons, "Diffusion theory of imprisonment of atomic resonance radiation at low opacities," *J. Phys. Chem.*, vol. 80, no. 7, pp. 653–659, Mar. 15, 1976.
[61] E. W. Samson, "Effects of temperature and nitrogen pressure on the afterglow of mercury resonance radiation," *Phys. Rev.*, vol. 40, no. 6, pp. 940–964, Jun. 15, 1932.
[62] C. Kenty, "On radiation diffusion and rapidity of escape of resonance radiation from a gas," *Phys. Rev.*, vol. 42, no. 6, pp. 823–842, Dec. 15, 1932.
[63] G. G. Lister, J. E. Lawler, W. P. Lapatovich, and V. A. Godyak, "The physics of discharge lamps," *Rev. Mod. Phys.*, vol. 76, no. 2, pp. 541–598, 2004.
[64] W. L. Morgan and L. A. Rosocha, "Water treatment and power cogeneration using hydrothermal, super critical water produced by pulsed electric discharges," *Int. J. Plasma Environ. Sci.*, in press.
[65] S. B. Radovanov, M. R. Tripkovic', and I. D. Holclajtner-Antunovic', "Diagnostics of pulsed discharge plasma in electrolyte," *Contrib. Plasma Phys.*, vol. 26, no. 6, pp. 389–397, 1986.
[66] S. B. Radovanov, I. D. Holclajtner-Antunovic', and M. R. Tripković, "On plasma composition of a pulsed discharge in electrolyte," *Plas. Chem. Plasma Process.*, vol. 6, no. 4, pp. 457–476, Dec. 1986.
[67] A. Starikovskiy, Y. Yang, Y. I. Cho, and A. Fridman, "Non-equilibrium plasma in liquid water: Dynamics of generation and quenching," *Plasma Sources Sci. Technol.*, vol. 20, no. 2, pp. 024003-1–024003-7, Apr. 2011.
[68] N. Y. Babaeva and M. J. Kushner, "Structure of positive streamers inside gaseous bubbles immersed in liquids," *J. Phys. D, Appl. Phys.*, vol. 42, no. 13, pp. 132003-1–132003-5, 2009.
[69] B. S. Sommers, J. E. Foster, N. Y. Babaeva, and M. J. Kushner, "Observations of electric discharge streamer propagation and capillary oscillations on the surface of air bubbles in water," *J. Phys. D, Appl. Phys.*, vol. 44, no. 8, pp. 082001-1–082001-6, Mar. 2001.
[70] N. Skoro, D. Marić, G. Malović, W. G. Graham, and Z. L. Petrović, "Electrical breakdown in water vapor," *Phys. Rev. E, Stat. Nonlineir Soft Matter Phys.*, vol. 84, no. 5, pp. 055401(R)-1–055401(R)-4, Nov. 2011.
[71] Y. Sakawa, K. Sugiyama, T. Tenabe, and R. More, "Fireball generation in a water discharge," *Plasma Fusion Res., Rapid Commun.*, vol. 1, pp. 039-1–039-2, 2006.
[72] A. Versteegh, K. Behringer, U. Fantz, B. Juttner, and S. Noack, "Long-living plasmoids from an atmospheric water discharge," *Plasma Sources Sci. Technol.*, vol. 17, no. 2, pp. 024014-1–024014-8, May 2008.

[73] N. Hayashi, H. Satomi, T. Kajiwara, and T. Tanabe, "Properties of ball lightning generated by a pulsed discharge on surface of an electrolyte in the atmosphere," *IEEJ Trans. Elect. Electron. Eng.*, vol. 3, no. 6, pp. 731–733, Nov. 2008.
[74] N. Hayashi, H. Satomi, T. Mohri, T. Kajiwara, and T. Tanabe, "General nature of luminous body transition produced by pulsed discharged on an electrolyte solution in the atmosphere," *IEEJ Trans. Elect. Electron. Eng.*, vol. 4, no. 5, pp. 674–676, Sep. 2009.
[75] G. A. Wurden, Z. Wang, C. Ticos, and C. J. v Wurden, "Free-floating atmospheric pressure ball plasmas," Los Alamos, NM, Los Alamos Report LA-UR-08-06284, 2008.
[76] R. Roy, M. L. Rao, and J. Kanzius, "Observations of polarized RF radiation catalysis of dissociation of $H_2O-NaCl$ solutions," *Mater. Res. Innov.*, vol. 12, no. 1, pp. 3–6, Mar. 2008.
[77] J. Kanzius and R. Roy, "RF systems and methods for processing salt water," WIPO Patent No. WO-2008/064002-AZ, May 29, 2008.
[78] J. Kanzius, W. H. Steinbrink, R. McDonald, and M. J. Keating, "Systems and methods for RF-induced hyperthermia using biological cells and nano particles as RF enhancer carriers," US Patent Appl. No. 20 050 251 234, Nov. 10, 2005.

W. Lowell Morgan (M'97) received the B.S.E. degree in physics and the B.S.E. degree in chemical engineering (with a minor in English) from the University of Michigan, Ann Arbor, in 1969 and the Ph.D. degree in physics from the University of Windsor, Windsor, ON, Canada, in 1976.

He performed postdoctoral research on metal-vapor–excimer plasmas with the Joint Institute for Laboratory Astrophysics, University of Colorado, Boulder, and then returned in 1987–1989 as a Visiting Fellow and Acting Director of the atomic and molecular data center. Between 1979 and 1987, he was a Staff Physicist with the Theoretical Atomic and Molecular Physics Group in the laser and weapons programs at the Lawrence Livermore National Laboratory and a Lecturer with the University of California, Davis. He is with Kinema Research & Software, LLC, Monument, which he founded in 1987. Since the mid-1980s, he has been a Visiting Scholar with AT&T Bell Laboratories; the University of Bari, Bari, Italy; Universite Paul Sabatier, Toulouse, France; Queen's University Belfast, Belfast, U.K.; the Australian National University, Canberra, Australia; the Center for Astrophysics, Harvard University, Cambridge, MA; and The Flinders University of South Australia, Adelaide, Australia. He has published research in the fields of plasma chemistry, laser physics, laser-produced plasmas, plasma processing chemistry, atomic and molecular physics, atmospheric chemistry, artificial neural networks, and astrophysics.

Dr. Morgan is a member of the American Physical Society, the American Chemical Society, the American Vacuum Society, and AAAS.

Louis A. Rosocha (A'94) received the B.S. degree in physics from the University of Arkansas, Fayetteville, in 1972 and the M.S. and Ph.D. degrees in physics (minor in chemistry) from the University of Wisconsin, Madison, in 1975 and 1979, respectively.

From 1978 to 1981, he was with the National Research Group of Madison, developing pulsed ultraviolet lasers, fast pulsed-power switchgear, and modeling commercial ozone generators. From October 1981 to January 2008, he was a Technical Staff Member and Manager with the Los Alamos National Laboratory (LANL). After an early retirement from LANL in 2008, he became an Independent Consultant with Applied Physics Consulting, Los Alamos, NM, focusing his R&D interests on CO_2 sequestration/global warming, national energy security, and water/air pollution abatement.

Dr. Rosocha is currently a member of the American Physical Society and Phi Beta Kappa.